Stanford Exploration Project, Report 103, April 27, 2000, pages 123–139

Short Note

Common-azimuth migration and Kirchhoff migration for 3-D prestack imaging: A comparison on North Sea data

Louis Vaillant[1] *and Henri Calandra*[2]

INTRODUCTION

Common-azimuth migration (CAM) is a 3-D prestack depth migration technique based on the wave equation (Biondi and Palacharla, 1996). It exploits the intrinsic narrow-azimuth nature of marine data to reduce its dimensionality and thus manages to cut the computational cost of 3-D imaging significantly enough to compete with Kirchhoff methods. Based on a recursive extrapolation of the recorded wavefield, CAM is potentially better able to handle multi-pathing problems induced by complex velocity structures.

Elf Aquitaine provided us with an interesting dataset recorded in the North Sea, which shows a salt dome and other 3-D structures. The complexity of the wave propagation in the medium, resulting from high lateral and longitudinal velocity contrasts, yields multi-pathing and illumination problems. Vaillant and Sava (1999) have already illustrated how this model is both a serious challenge for imaging and an interesting test case for the CAM method.

In this paper, we present our latest imaging results that cover the whole vertical extent of the salt body with the CAM technique, as a complementary study to Vaillant and Sava (1999). At the same time, we compare the CAM-migrated cube to the image obtained using a state-of-the-art Kirchhoff algorithm and discuss the specificities of both approaches.

PREPROCESSING AND COMMON-AZIMUTH MIGRATION

The wave-equation approach obliges us to transform the 3-D data acquired with complex irregular geometry to regularly space-sampled data because CAM operates in the frequency-wavenumber domain and requires Fourier transforms along all axes. In contrast, Kirchhoff algorithms can handle irregular geometries without such preprocessing because they operate sequentially in a trace-by-trace manner.

[1]**email:** louis@sep.stanford.edu
[2]Elf Exploration Production, Pau, France
email: henri.calandra@elf-p.fr

Here, data regularization is performed by an operator called AMO or Azimuth Moveout (Biondi et al., 1998). It also allows a local coherent stack that will reduce data volume. AMO, however, has a non-negligible computational cost in the whole imaging process (about 10% of migration cost). Effectively, introduced as the cascade of DMO and inverse DMO, AMO is a partial migration operator. With less accuracy, one can instead use a simple normalized binning procedure.

The processing scheme begins by creating a 5-axis time-midpoint-offset grid $(t, \vec{m}, \vec{h})$ for the data volume. Then, we apply a simple sequence NMO/AMO/NMO^{-1} to regularize the data on the grid. This gridding procedure concurrently allows data resampling in common-midpoint and offset at the limit of aliasing, thus reducing further the cube dimensions and lower migration computational cost.

Marine data are usually concentrated within a narrow range of azimuth, as opposed to land data. Here, besides regularizing data along space axes, we use AMO to sum data coherently over the cross-line offset axis h_y; conventionally, the subscripts x and y refer to the in-line and the cross-line direction, respectively. Thus, we obtain 4-D common-azimuth data, for which $h_y = 0$. After transformation to the frequency-wavenumber domain, this 4-D common-azimuth regularized dataset $D(\omega, \vec{k_m}, k_{hx})$ is the wavefield recorded at depth $z = 0$, to which CAM is applied.

Migration is then performed iteratively through common-azimuth downward-continuation of the wavefield (Biondi and Palacharla, 1996). The common-azimuth downward-continuation operator is derived from the stationary-phase approximation of the full 3-D prestack downward continuation operator. For more accuracy with lateral velocity variations, we use several reference velocities and interpolation as in the extended split-step method (Stoffa et al., 1990). The following chart summarizes the preprocessing and imaging schemes:

$$
\begin{aligned}
\widetilde{D}_{irr}(t) &= \text{Gridding} \Rightarrow & \widetilde{D}\left(t, \vec{m}, \vec{h}\right) \\
\widetilde{D}\left(t, \vec{m}, \vec{h}\right) &= \text{AMO} \Rightarrow & D\left(t, \vec{m}, hx\right) \\
D_{z=0}\left(\omega, \vec{k_m}, k_{hx}\right) &= \text{Down} \Rightarrow & D_z\left(\omega, \vec{k_m}, k_{hx}\right) \\
D_z\left(\omega, \vec{k_m}, k_{hx}\right) &= \text{Imaging} \Rightarrow & D_z\left(\tau = 0, \vec{m}, h_x = 0\right)
\end{aligned}
$$

In this chart, $\widetilde{D}$ refers to data as an irregular set of traces, whereas D means data are a regular n-D cube.

APPLICATION TO REAL DATA

The migrated volume covers an area of 10.5×4km, down to 5km. The velocity model, courtesy of Elf Aquitaine, was obtained by reflection tomography using the SMART method (Jacobs et al., 1992). For migration, we used 6 reference velocities and interpolation in an extended split-step manner. With data dimensions indicated in Table 1, the 3-D prestack common azimuth migration ran in 40 days on 4 processors of our SGI Power Challenge (18 MIPS R8000 processors).

Table 1: number of samples

Cmp-X	Cmp-Y	Depth	Offset	Frequencies	Velocities
525	160	400	64	176	6

Figure 1 shows a typical set of sections in the middle of the migrated cube. In the in-line section, the shallower part (above 1500m) reveals high-frequency details accurately imaged: the migration enhanced a graben structure, with normal faults and rotated blocks, around location Cmp-X=8000m, close to the top. The horizontal section at depth 900m highlights complex patterns inside sedimentary layers, imaged with a high resolution, that can be interpreted as turbidite channels. The imaging of the salt body is satisfactory, with sediments clearly bent towards the salt flank on the left-hand side. The salt flank itself has not been well focused, but can be revealed by residual migration (Sava, 2000). Even with an imperfect velocity model, migration enhances deep layers and most of the bottom of the salt. Several layers below the salt are also well focused.

COMPARISON WITH KIRCHHOFF MIGRATION

Figures 3 and 4 show comparisons between CAM and Kirchhoff migration results. The Kirchhoff algorithm used is derived from a preserved-amplitude approach and selects the most energetic arrival. Both CAM and Kirchhoff migration use exactly the same velocity model.

Some of the most significant differences between both approaches are well-known: in the CAM algorithm, finite frequency wave propagation is modeled avoiding the asymptotic approximations necessary for Kirchhoff. Also, for deep targets, the migration cost increases as N_z^3 (number of depth samples) for Kirchhoff, whereas CAM cost only increases as N_z^2. However, Kirchhoff methods allow target-oriented migrations where CAM has to perform downward-continuation of the whole wavefield.

Figure 4 shows that the in-line sections around the salt body are relatively comparable in quality. Globally, CAM seems to give better results at imaging sediments bending against the salt flank on the left-hand side. The most important differences are shown by the horizontal sections (Figure 3): at a depth of 900m, CAM enhances complex high-frequency turbiditic patterns in shallow layers. At the same location, the Kirchhoff image appears at a considerably lower frequency and blurred along the in-line direction.

There are potentially 3 factors that could explain CAM's better accuracy compared to Kirchhoff migration:

- Wave propagation is handled completely differently: CAM iteratively propagates the wavefield by regular depth steps, as opposed to Green functions for Kirchhoff that are evaluated by ray tracing, wavefront construction or other methods.

- Since Green functions are not calculated for every source but rather pre-computed on a coarser grid, Kirchhoff algorithms usually include critical interpolations of traveltime

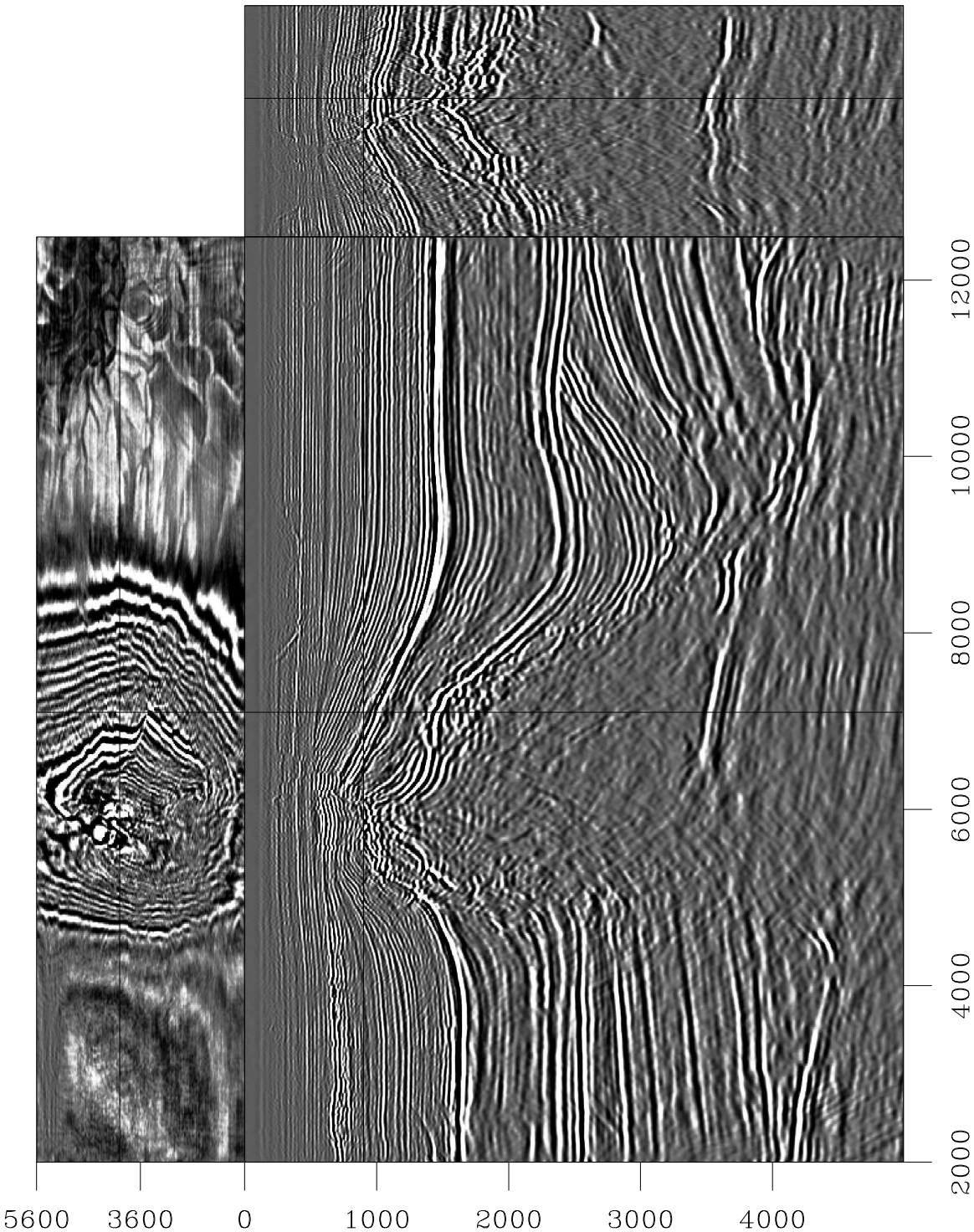

Figure 1: Sections of the image cube migrated with CAM: in-line Cmp-Y=4000m (center), depth slice z=900m (top), cross-line at Cmp-X=7100m (side). louis2-L7d-image-all-2 [CR]

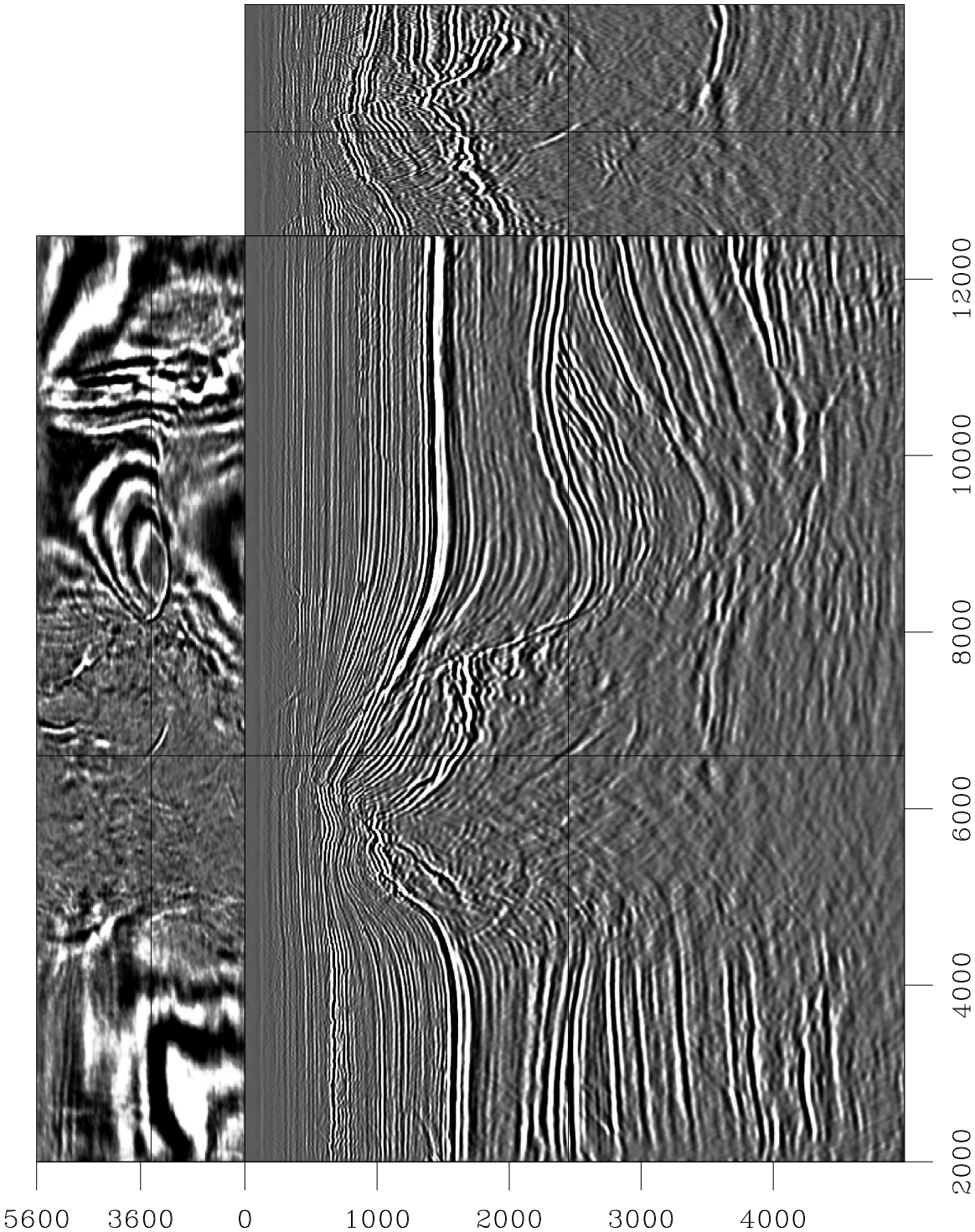

Figure 2: Sections of the image cube migrated with CAM: in-line Cmp-Y=3400m (center), depth slice z=2450m (top), cross-line at Cmp-X=6600m (side). louis2-L7d-image-all-2bis [CR]

maps and other attributes that may reduce accuracy for high-frequency details in the image. The only interpolations performed with CAM are the extended split-step scheme, which essentially addresses rapid velocity variations.

- Even if Kirchhoff algorithms can easily handle irregular geometries, the resulting image incorporates acquisition footprints, especially in depth slices. On the contrary, CAM requires regular geometry and acquisition problems are addressed during preprocessing through the AMO operator. Thus, the whole imaging stage is done with regularized geometry and potentially enables higher resolution in the final image.

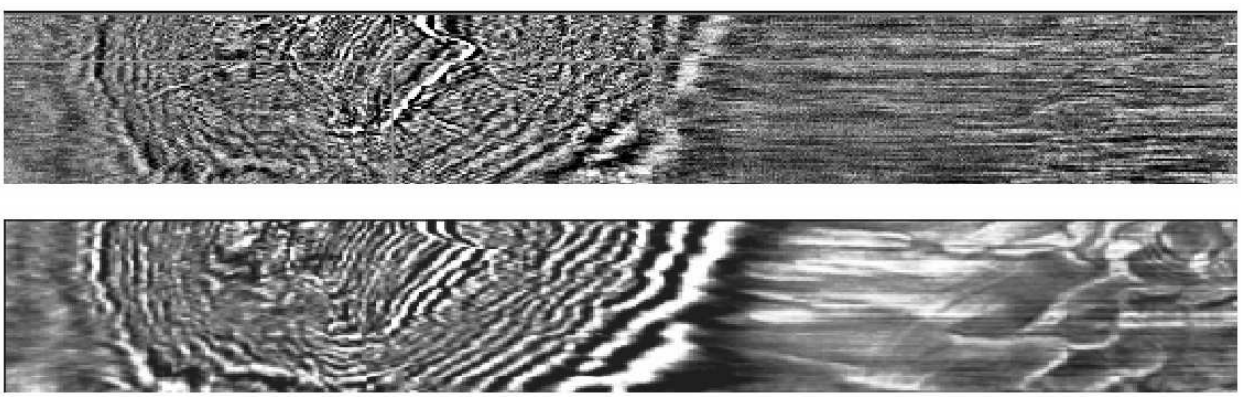

Figure 3: Comparison between Kirchhoff (top) and CAM (bottom) imaging results: depth slice at z=900m. The Kirchhoff image has a lower frequency content, a higher noise ratio and is blurred along the in-line direction. louis2-kir-cam-zslice [NR]

CONCLUSION

Real data offer an opportunity to test our imaging techniques further. Common-azimuth migration (CAM) is an attractive method for seismic imaging in complex media and it remains a subject for further research. Its computational cost and its high resolution in depth slices, illustrated in this particular example, can make it an attractive alternative to widespread Kirchhoff methods. Both approaches show different specificities and are equivalently valuable in our seismic imaging toolbox.

REFERENCES

Biondi, B., and Palacharla, G., 1996, 3-D prestack migration of common-azimuth data: Geophysics, **61**, no. 6, 1822–1832.

Biondi, B., Fomel, S., and Chemingui, N., 1998, Azimuth moveout for 3-D prestack imaging: Geophysics, **63**, no. 2, 574–588.

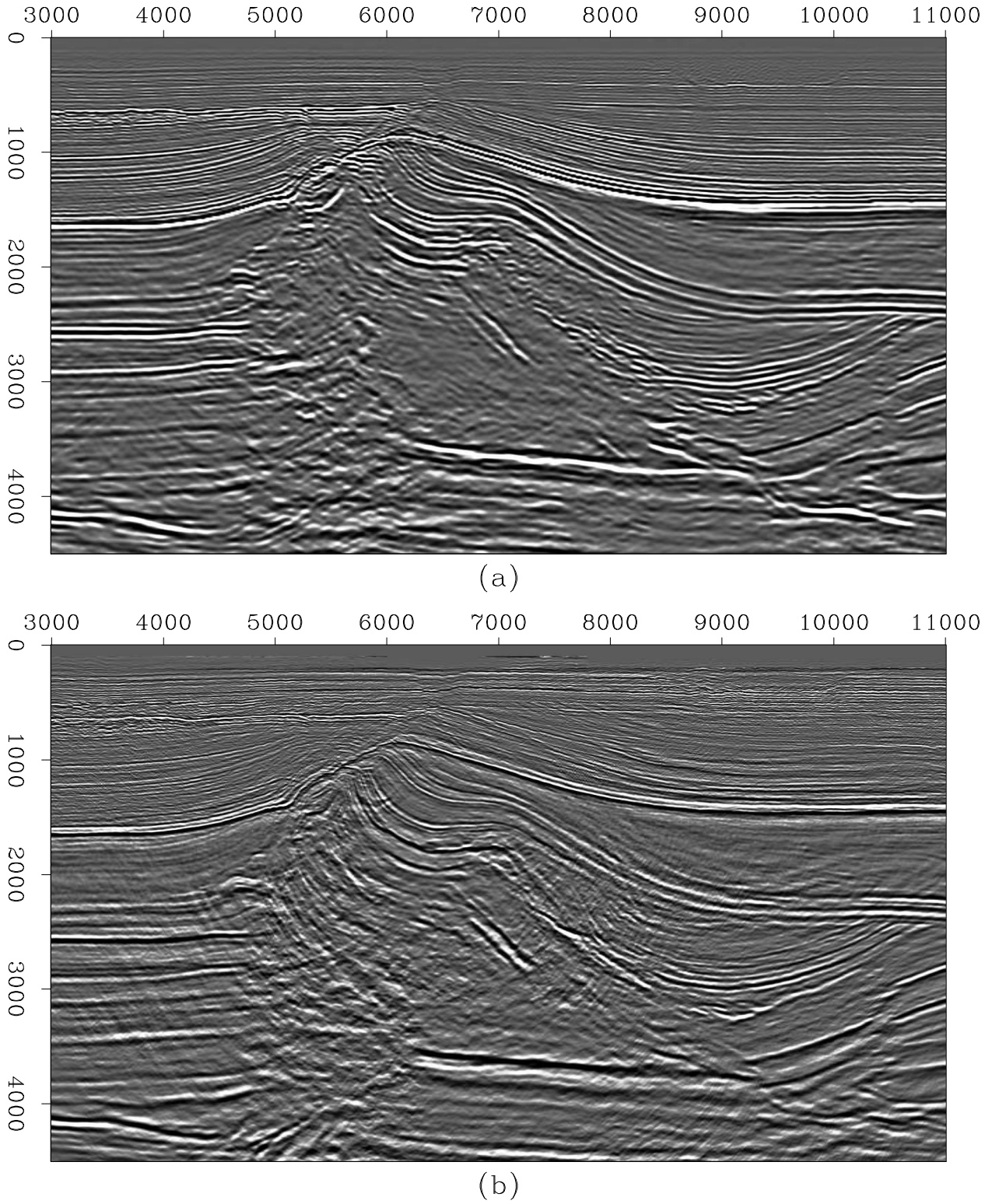

Figure 4: Comparison between CAM (a) and Kirchhoff (b) imaging results for the in-line section at Cmp-Y=3250m. louis2-xz-CAM-KIR [CR]

Jacobs, J. A. C., Delprat-Jannaud, F., Ehinger, A., and Lailly, P., 1992, Sequential migration-aided reflection tomography: A tool for imaging complex structures: 62nd Annual Internat. Mtg., Soc. Expl. Geophys., Expanded Abstracts, 1054–1057.

Sava, P., 2000, Variable-velocity prestack Stolt residual migration with application to a North Sea dataset: SEP–**103**, 147–157.

Stoffa, P. L., Fokkema, J. T., de Luna Freire, R. M., and Kessinger, W. P., 1990, Split-step Fourier migration: Geophysics, **55**, no. 4, 410–421.

Vaillant, L., and Sava, P., 1999, Common-azimuth migration of a North Sea dataset: SEP–**102**, 1–14.